

Short Communication

Improved Electrochromic Performance in Nickel Oxide Thin Film by Zn Doping

Kyung Ho Kim*, Mei Kahuku, Yoshio Abe, Midori Kawamura, Takayuki Kiba

Department of Materials Science and Engineering, Kitami Institute of Technology, 165 Koen-cho, Kitami, Hokkaido 090-8507, Japan

*E-mail: khkim@mail.kitmai-it.ac.jp

Received: 4 January 2020 / Accepted: 10 February 2020 / Published: 10 April 2020

Zn-doped NiO thin films were prepared using the simple sol-gel spin-coating method and their electrochromic characteristics were compared with undoped NiO thin film. The transparency in the visible region and uniformity of the NiO thin films were enhanced with increasing Zn doping amounts. The *in situ* optical transmittance spectra revealed all samples were transparent at bleached state, whereas the color changed from light brown to dark brown at a colored state, as the Zn doping amounts increased. The Zn-doped NiO thin film exhibited a higher transmittance change (ΔT) of 59.8% and higher color efficiency (CE) of 33.6 cm²/C at a wavelength of 500 nm compared with the undoped film (22.4% (ΔT) and 27.3 cm²/C (CE)). Moreover, it displayed a sustained memory effect under open circuit. The addition of the Zn dopant offered a simple way to improve the electrochromic performance of the NiO thin film.

Keywords: NiO, Zn dopant, Thin film, Electrochromic performance

1. INTRODUCTION

The wide bandgap nickel oxide (NiO) nanostructures serving as anodic electrochromic material for smart windows have been intensively studied. The electrochromic performance of the NiO films exhibits a strong dependence on the porosity, film thickness, annealing treatment condition, and crystallinity [1-5]. Usually, a porous and thick NiO film annealed at a proper temperature displays a better electrochromic performance compared to one that is compact and thin. Pereira *et al.* reported that as the film thickness increased from 100 to 500 nm, the thicker NiO film prepared by e-beam evaporation showed enhanced electrochromic performance [3]. Xia *et al.* reported that a porous NiO film annealed at 300 °C had better than those annealed at 350 °C and 400 °C [4]. In addition, the incorporation of a dopant (e.g., Cu, Zn, and Al) was a plausible way to alter the properties of NiO thin films [6-11]. In

previous paper, we reported that the effects of a Cu dopant on the morphological and electrical properties of NiO thin films prepared by sol-gel that had the merits of being large-area production and easy composition control [7]. He *et al.* reported that the electrochromic performance of Cu-doped NiO thin film was better than that of undoped NiO prepared by sol-gel dip-coating [8]. The optical and electrical properties of Zn-doped NiO had also received significant attention. Manouchehri *et al.* noted that the optical band gap and crystallite size of NiO prepared by RF sputtering decreased with increasing Zn doping amounts [9]. Furthermore, NiO-based films are reported to display an ozone-induced coloration property [10]. However, studies on the electrochromic characteristics of the Zn-doped NiO thin film remain limited [11].

In this study, we investigate the morphological and electrochromic properties of 120-nm-thick NiO films prepared by the sol-gel spin-coating method with the addition of a Zn dopant. The incorporation of the Zn dopant provided a simple way to improve the electrochromic performance of the NiO thin film.

2. EXPERIMENTAL

For the preparation of sol, nickel acetate tetrahydrate (Ni(Ac), $\text{Ni}(\text{CH}_3\text{COO})_2 \cdot 4\text{H}_2\text{O}$, 0.5 M) was dissolving in 2-methoxyethanol (2ME, $\text{C}_3\text{H}_8\text{O}_2$), followed by the addition of zinc acetate dihydrate (Zn(Ac), $\text{Zn}(\text{CH}_3\text{COO})_2 \cdot 2\text{H}_2\text{O}$, 0.05-0.10 M) as a dopant. The mixture was stirred at 60 °C for 1 h and aged at room temperature for 24 h. Spin-coating was performed at 2100 ~ 2400 rpm to adjust the film thickness, accompanied by drying at 100 °C for 10 min. The spin-coating and dry processes were repeated, followed by annealing at 300 °C for 1 h in air. The nanostructure samples produced were named 0NZO, 5NZO, and 10NZO with Zn(Ac) contents of 0, 0.05, and 0.10 M, respectively.

The crystalline phase was characterized by X-ray diffraction (XRD, D8ADVANCE). The film morphology was examined by field emission scanning electron microscope (FESEM, JSM-6701). The optical transmittance spectra were obtained from ultraviolet-visible (UV-Vis) spectroscopy (HITACHI, U-2910). The chemical bonding state was identified by Fourier transform infrared spectroscopy (FTIR, FT/IR-6100). Cyclic voltammetry (CV) measurements were conducted between -0.50 and 0.55 V at a scan rate of 10 mV/s with Pt and Ag/AgCl used as the counter and the reference electrodes, respectively. The *in situ* optical transmittance spectra were measured using a charge-coupled device multichannel detector (USB2000+, Ocean Optics) and halogen and deuterium lamps. For the *in situ* transmittance measurements, air and a quartz-glass cell filled with 1M KOH aqueous electrolyte were used as references [12].

3. RESULTS AND DISCUSSION

Figure 1(a) shows XRD patterns of the sample containing different Zn(Ac) amounts. All samples display weak diffraction peaks at the 2θ positions of 37.3° and 43.3° indexed as the (111) and (200) planes, respectively, of the face-centered cubic NiO (JSPDS No.04-0835). No secondary phase

diffraction peaks associated with Ni, Zn, or ZnO are observed. The solubility of Zn on the NiO is known to be high [10,13], with Park *et al.* reporting that the crystalline structure of $Zn_{0.31}Ni_{0.69}O$ remained as a pure NiO phase with no secondary phase like ZnO [13]. Meanwhile, the intensities of the diffraction peaks decreased relatively, with the peak positions shifting to lower angles with increasing Zn(Ac) amounts. This characteristic is likely due to the ionic radius difference of Ni^{2+} (0.069 nm) and Zn^{2+} (0.074 nm) [10,14]. The FTIR spectra were shown in Fig.1(b). All NiO samples had a strong absorption peak at $\sim 400\text{ cm}^{-1}$ corresponding to Ni-O stretching vibration [4,15]. Furthermore, the broad absorption around 3400 cm^{-1} corresponds to the stretching hydroxyl groups hydrogen-bonded vibration of water [4,15]. The hydroxyl groups almost disappeared with increasing annealing temperature. The XRD and FTIR results indicate the formation of NiO. Figure 1(c) shows the optical transmittance spectra. With increasing Zn amounts, the average transmittance in the visible region increases and the absorption edge shifts to a short wavelength. From the inset in Fig.1(c), the optical band gap (E_g) calculated is 3.90, 3.96, and 4.00 eV for the 0NZO, 5NZO, and 10NZO samples, respectively, coherent with previous studies [16,17]. The results of the optical properties suggest that the average size of the nanoparticles decreased with increasing Zn amounts [17].

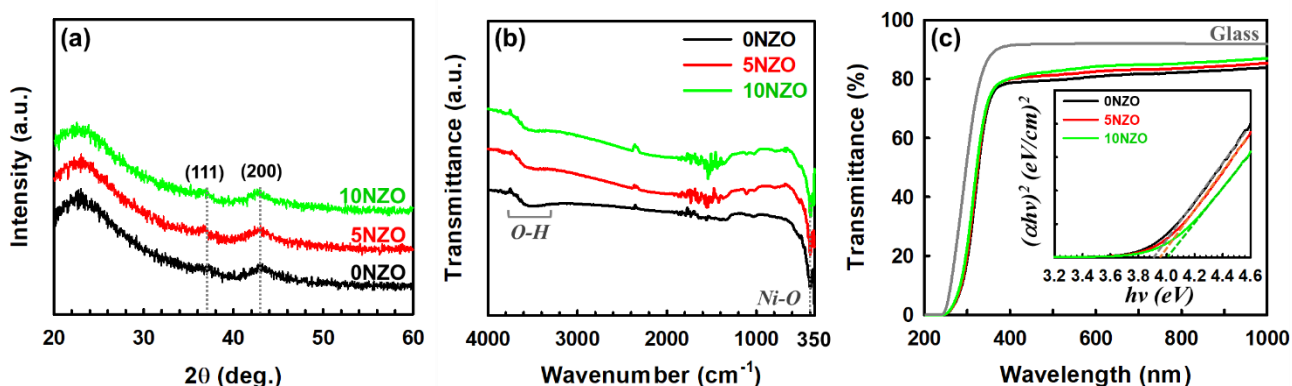


Figure 1. XRD patterns (a), FTIR spectra (b), and optical transmittance (c) of the NiO thin films with different Zn amounts; the inset in (c) plots $(\alpha hv)^2$ vs hv .

Figure 2(a-c) displays cross-sectional FESEM images of the NiO samples prepared on fluorine-doped tin oxide (FTO with film thickness $\sim 550\text{ nm}$) coated glass substrate with different Zn amounts. The average film thickness is $\sim 120\text{ nm}$, with cracks (indicated by arrows) observed on the 0NZO thin film that was exposed to the bare surface of the FTO substrate. The proportion of cracks increased as the annealing temperature increased. This is attributed to likely because high residual stress of the NiO film [18]. The effective release of such stress improved the film uniformly with the addition of Zn as demonstrated in Fig.2(d-f).

Figure 3(a-c) shows the *in situ* transmittance variation (ΔT) at a wavelength of 500 nm of the 0NZO, 5NZO, and 10NZO samples at a scan rate of 10 mV/s. The obtained optical density (ΔOD , $\Delta OD = \log(T_{\text{bleached}}/T_{\text{colored}})$) are presented in Fig.3(d).

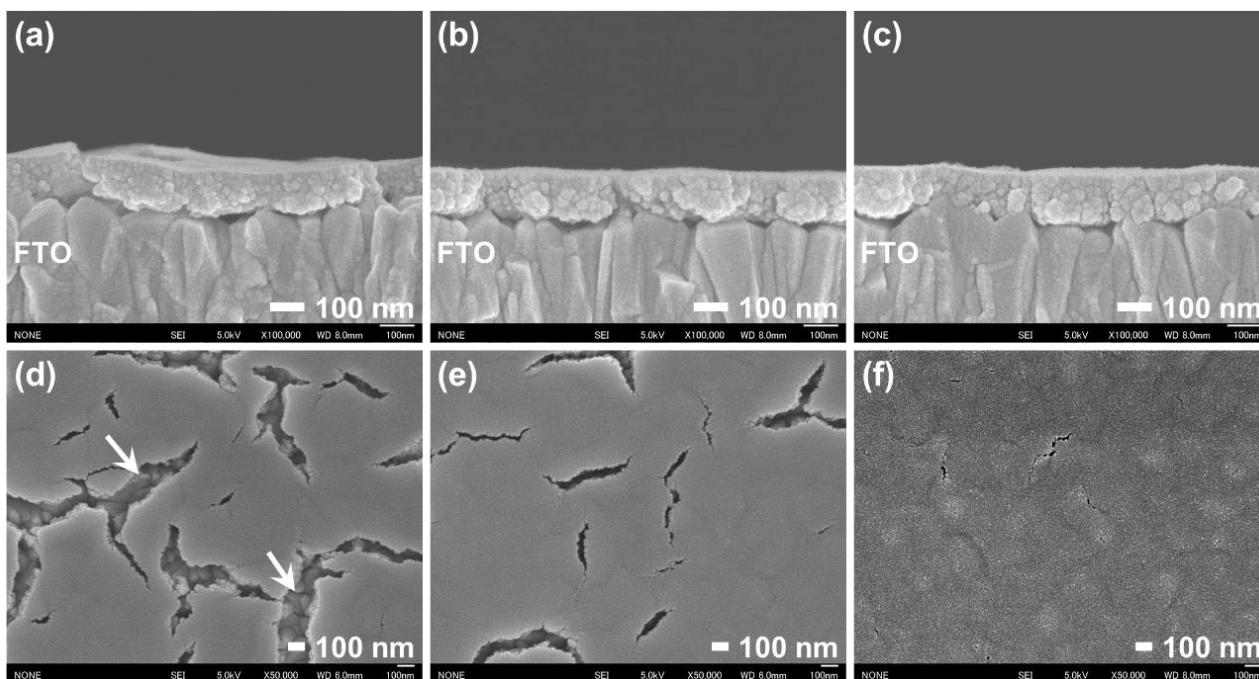


Figure 2. Cross-sectional (a-c) and top view (d-f) FESEM images of the NiO thin films with different Zn amounts; (a,d) 0NZO, (b,e) 5NZO, (c,f) 10NZO.

The undoped NiO (0NZO) sample shows stable transmittance change up to 20,000 s with of ΔT and ΔOD of 22.4% and 0.15, respectively, representing reasonable performance compared to others reported [3,19,20]. After the CV measurement, no film detachment from the FTO substrate was observed. With the addition of Zn, the *in situ* transmittance change gradually improves and even saturated at times (Fig.3(b,c)). The ΔT and ΔOD of the 10NZO are 59.8% and 0.55, respectively. At the bleached state, all samples are transparent, whereas, at the colored state, samples change from light brown to dark brown as the Zn amounts increased. Considering its film thickness (~120 nm), the 10NZO sample shows better performance than previously reported nano-porous NiO film prepared by sol-gel spin-coating method (4 cycles with thickness ~220 nm, ΔT ~30% at 500 nm wavelength) [20], and thick NiO film prepared by the sol-gel dip coating method (8 layers with thickness 445 nm, ΔT ~50% at 500 nm wavelength) [20]. After 20,000 s cycling process, the CV curves at a scan rate of 10 mV/s are shown in Fig.3(e). All samples show oxidation and reduction peaks associated with the coloration and bleaching states [5]. The extraction of protons and electrons from the thin film leads to coloration and reverse process leads to the bleaching. During cycling, the thin film changes from brown to transparent reversibly [4,5]. No significant difference emerges between the inserted (Q_{in}) and corresponding extracted (Q_{ex}) charge densities over all the samples; the Q_{in}/Q_{ex} ratio for the 0NZO, 5NZO, and 10NZO samples are 1.06, 1.05, and 1.03, respectively. Contrarily, the current density increased in the order of 0NZO, 5NZO, and 10NZO. This indicates that the quantity of ions and electrons inserted into the thin film also increases, implying that reaction activity of the Zn-doped NiO thin film is better than the undoped thin film [3]. This further supports the observation that electrochromic behavior is enhanced by the addition of Zn on NiO thin film. As shown in Fig.3(f), the calculated charge density (Q) and color

efficiency (CE, $CE = \Delta OD/Q$) increase with increasing Zn amounts, the 10NZO sample showing values of 15.6 mC/cm² and 33.6 cm²/C, respectively.

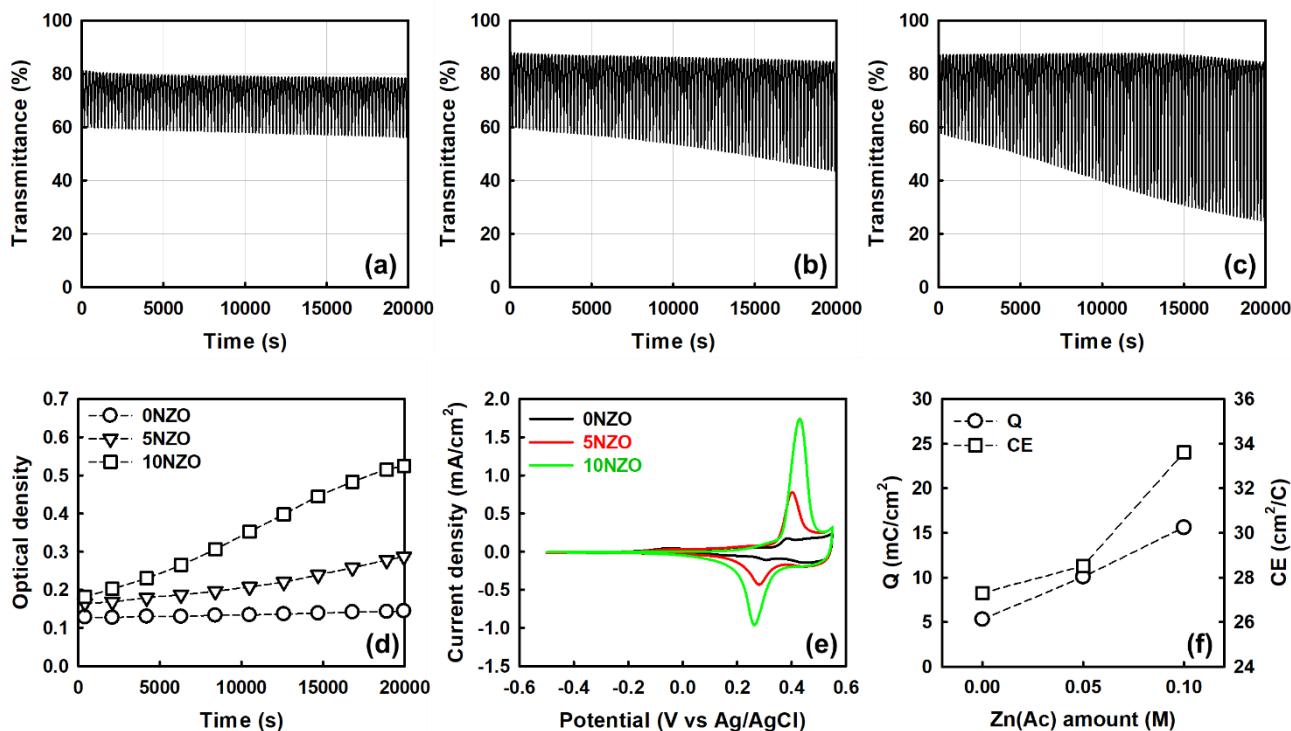


Figure 3. *In situ* transmittance change (a-c), optical density (d), CV curves (e), and calculated Q and CE (f); (a) 0NZO, (b) 5NZO, (c) 10NZO.

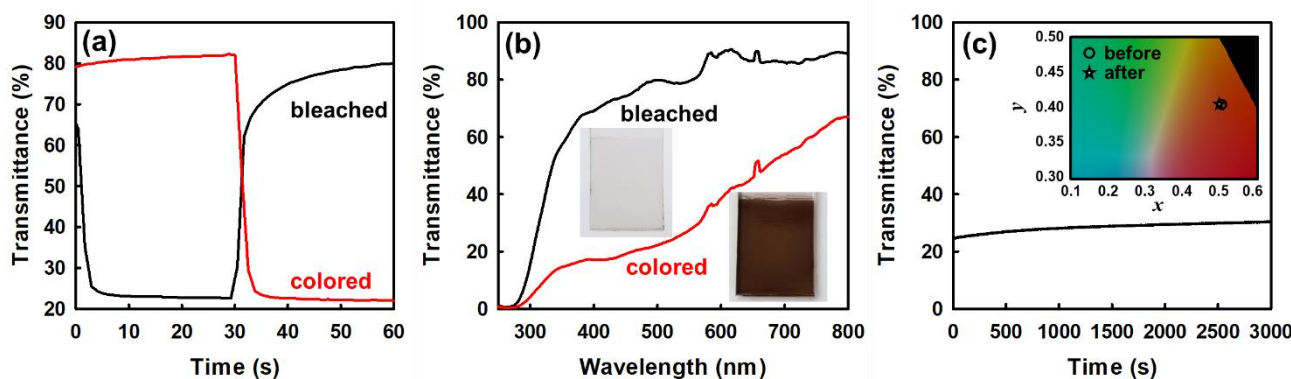


Figure 4. Response time measurements for the 10 NZO sample (a), transmittance spectra of the 10 NZO sample at bleached and colored states (b), and memory effect (c) of the 10NZO sample; the inset in (b) are photo images of the bleached and colored states, while the inset in (c) is the CIE 1931 Yxy chromaticity diagram.

From Fig.4(a), the response times at a wavelength of 500 nm, defined as the duration to reach 90% of the full change in transmittance [5], for the bleached state (@-0.50 V for 30 s) and colored state

(@+0.55 V for 30 s) are ~8 and ~3 s, respectively. The transmittance spectra of the 10NZO thin film with an applied potential of a colored and bleached state are shown in Fig.4(b). The color of the 10NZO changed from transparent in the bleached state to dark brown in the colored state. In addition, at the colored state, a variation of the *in situ* transmittance at a wavelength of 500 nm was measured under an open circuit condition (Fig.4(c)). Furthermore, before and after memory effect test, CIE 1931 Y_{xy} chromaticity diagram for the 10NZO sample is inserted, with no significant shift in x-y co-ordinates. This supports a sustained memory effect for the 10NZO sample.

4. CONCLUSIONS

We investigated the electrochromic performance of the 120 nm-thick NiO thin films prepared by the simple sol-gel spin-coating method with different Zn amounts. The average transmittance in the visible region and the E_g of the NiO thin films increased with increasing Zn amounts. The NiO thin film more uniformly covered on the surface of the FTO substrate with the incorporation of Zn, and improving electrochromic performance through high optical contrast, charge density, color efficiency.

ACKNOWLEDGEMENT

This study was partially supported by a Grant-in-Aid for Scientific Research (C) (No. 17K06336) from the Japan Society for the Promotion of Science.

References

1. P. Yang, P. Sun, and W. Mai, *Mater. Today*, 19 (2016) 394.
2. J. Zhang, J.P. Tu, X.H. Xia, Y. Qiao, and Y. Lu, *Sol. Energy Mater. Sol. Cells*, 93 (2009) 1840.
3. S. Pereira, A. Gonçalves, N. Correia, J. Pinto, L. Pereira, R. Martins, and E. Fortunato, *Sol. Energy Mater. Sol. Cells*, 120 (2014) 109.
4. X.H. Xia, J.P. Tu, J. Zhang, X.L. Wang, W.K. Zhang, and H. Huang, *Sol. Energy Mater. Sol. Cells*, 92 (2008) 628.
5. S. Hou, A.I. Gavriluk, J. Zhao, H. Geng, N. Li, C. Hua, K. Zhang, and Y. Li, *Appl. Surf. Sci.*, 451 (2018) 104.
6. H. Yang, J-H. Yu, H.J. Seo, R.H. Jeong, and J-H. Boo, *Appl. Surf. Sci.*, 461 (2018) 88.
7. K.H. Kim, C. Takahashi, Y. Abe, and M. Kawamura, *Optik*, 125 (2014) 2899.
8. Z. He, Z. Ji, S. Zhao, C. Wang, K. Liu, and Z. Ye, *Sol. Energy*, 80 (2006) 226.
9. I. Manouchehri, S.A.O. Alshiaa, D. Mehrparparvar, M.I. Hamil, and R. Moradian, *Optik*, 127 (2016) 9400.
10. R. Noonuruk, W. Techitdheera, and W. Pecharapa, *Thin Solid Films*, 520 (2012) 2769.
11. R. Noonuruk, W. Mekprasart, and W. Pecharapa, *Phys. Status Solidi C*, 12 (2015) 560.
12. Y. Abe, S. Yamauchi, M. Kawamura, K.H. Kim, and T. Kiba, *J. Vac. Sci. Technol. A*, 36 (2018) 02C102.
13. Y.R. Park, and K.J. Kim, *J. Cryst. Growth*, 258 (2003) 380.
14. İ.Y. Erdoğan, *J. Alloy. Compd.*, 502 (2010) 445.

15. M. Arif, A. Sanger, M. Shkir, A. Singh, and R.S. Katiyar, *Physica B*, 552 (2019) 88.
16. S. Akinkuade, B. Mwankemwa, J. Nel, and W. Meyer, *Physica B*, 535 (2018) 24.
17. A.K. Srivastava, S. Thota, and J. Kumar, *J. Nanosci. Nanotechnol.*, 8 (2008) 4111.
18. D. Evecan, Q. Gurcuoglu, and E.O. Zayim, *Microelectronic Eng.*, 128 (2014) 2.
19. W.C. Lee, E.C. Choi, J-H. Boo, and B. Hong, *Thin Solid Films*, 641 (2017) 28.
20. K.K. Purushothaman, S. Joseph Antony, and G. Muralidharan, *Sol. Energy*, 85 (2011) 978.

© 2020 The Authors. Published by ESG (www.electrochemsci.org). This article is an open access article distributed under the terms and conditions of the Creative Commons Attribution license (<http://creativecommons.org/licenses/by/4.0/>).